JOURNAL OF SCIENCE AND TECHNOLOGY
ISSN: 2229-8460 e-ISSN: 2600-7924

JST

Vol. 17 No. 1 (2025) 108-120
https://publisher.uthm.edu.my/ojs/index.php/jst

Morphology and Physiochemical Characterization of Perfluorosulfonic Acid (PFSA) Membrane for Electrochemical Application

Mohd Hafiz Md Ali[1], Mohammad Noor Jalil[1]*, Mohamad Nor Amirul Azhar Kamis[1], Hamizah Mohd Zaki[1]

[1] *School of Chemistry and Environment, Faculty of Applied Science, Universiti Teknologi MARA, Shah Alam, 40000, Selangor MALAYSIA*

*Corresponding Author: moham423@uitm.edu.my
DOI: https://doi.org/10.30880/jst.2025.17.01.011

Article Info

Received: 11 September 2024
Accepted: 17 May 2025
Available online: 30 June 2025

Keywords

Perfluorosulfonic acid (PFSA), morphology, chemical, physiochemical

Abstract

This report provides a thorough examination of the surface morphology, chemical content, and physical properties of Perfluorosulfonic Acid (PFSA) membrane which is commonly utilised as a conductive membrane in fuel cells, ionic batteries, and electrolysers. This experimental effort is separated into two parts: morphological characterisation and physicochemical analysis, which aim to improve understanding of the membrane functional qualities. The membrane surface and cross-sectional characteristics were examined at varied magnifications using Field Emission Scanning Electron Microscopy (FESEM) and Energy-Dispersive X-ray Spectroscopy (EDX). The EDX results revealed that the membrane surface is predominantly composed of carbon (C), oxygen (O), manganese (Mn), and nickel (Ni), accounting for 22.82% by mass, whereas the cross-section analysis revealed higher mass percentages of titanium (Ti), sulphur (S), oxygen (O), carbon (C), and fluorine (F), totalling 53.51%. Tensile testing confirmed the membrane's strength, with a tensile stress of 13.71 N/mm^2 and an elongation at break of 73.73%. Thermal stability and breakdown behaviour were determined using Thermogravimetric Analysis (TGA), which validated this membrane thermal endurance at 422^{o}C degradation temperatures. These findings provide significant understanding into the surface morphology and structural functional features of PFSA membrane which allow its optimisation for advanced electrochemical applications.

1. Introduction

Perfluorosulfonic acid (PFSA) membrane, employed in proton exchange membrane (PEM) fuel cells, demonstrate a distinctive set of properties essential for optimal performance in electrochemical applications[1].This membrane shows high proton conductivity, exceptional chemical and thermal stability, and mechanical strength, rendering it suitable in various applications such as fuel cells, electrolyser and redox flow batteries[2]. PFSA membranes play a crucial role in electrochemical devices, particularly in proton exchange membranes (PEMs) for fuel cells and electrolysers. Instead of that, its nanostructured morphology influences proton conductivity, mechanical strength, and chemical stability[3]. These unique design of PFSA membranes, consisting of hydrophobic polytetrafluoroethylene (PTFE) backbones and hydrophilic sulfonic acid side chains, is key to

achieving high proton conductivity. Due to that characteristic, PFSA membranes offer high proton conductivity, a critical characteristic for optimal performance in fuel cells, which the membrane serves as a pathway for proton transport while ensuring gas separation[4]. The presence of sulfonic acid groups in the PFSA polymer structure is responsible for high proton conductivity, as these groups attract water molecules and enhance ion transport [5].The polymer structure, including the reduction of side chains or the incorporation of other materials, have demonstrated improvements in conductivity and dimensional stability during operational conditions. This unique structure is key to achieving high proton conductivity, which is essential for efficient fuel cell performance. Research highlights that the connectivity and size of these hydrophilic domains are vital to the water content and overall performance of the membranes [6].The morphology of the hydrated states in PFSA membranes has been shown to consist of water clusters that facilitate proton conduction, demonstrating the importance of structural characteristics in enhancing ionic transport pathways[7].

The chemical properties shows the stability of PFSA membranes in harsh operational environments because it exhibit resilience against degradation by radical species, especially in low humidity and high-temperature conditions typical of fuel cell and electrolyser conditions Despite being stable at high temperatures (up to 130 °C), PFSA membranes still have problems with hydroxyl radical-induced breakdown at low humidity levels [8].However, the addition of zirconium phosphate improves the mechanical properties of PFSA membranes while maintaining their chemical integrity . The mechanical strength and dimensional stability are important characteristics of PFSA membranes, essential for the longevity and durability of fuel cells. Studies demonstrate that the incorporation of nanofibers and composite structures improves the mechanical integrity and structural stability of PFSA membranes [9].

This study focuses on the morphology of PFSA membranes using FESEM imaging to observe their microstructure, which may reveal key variables influencing performance. Additionally, EDX analysis is employed to detect the presence of specific elements that contribute to increased ion conductivity. Previous studies have shown that highly ordered PFSA membranes can effectively minimize ion crossover and improve performance metrics in applications such as vanadium redox flow batteries .The configuration of ion channels and the spatial distribution of water clusters within the membrane significantly influence its transport properties, which are critical for overall application efficiency[10].Furthermore, the physical properties of PFSA membranes can be evaluated through tensile and TGA testing, providing a more comprehensive understanding of their structural and thermal characteristics.

2. Materials

Perfluorosulfonic acid (PFSA) membrane type Nafion 115 was purchased from Sigma-Aldrich with formula ($C_7HF_{13}O_5S$. C_2F_4)x. The chemical structure for PFSA membrane was illustrated in Fig.1. The chemical used is received unless otherwise stated.

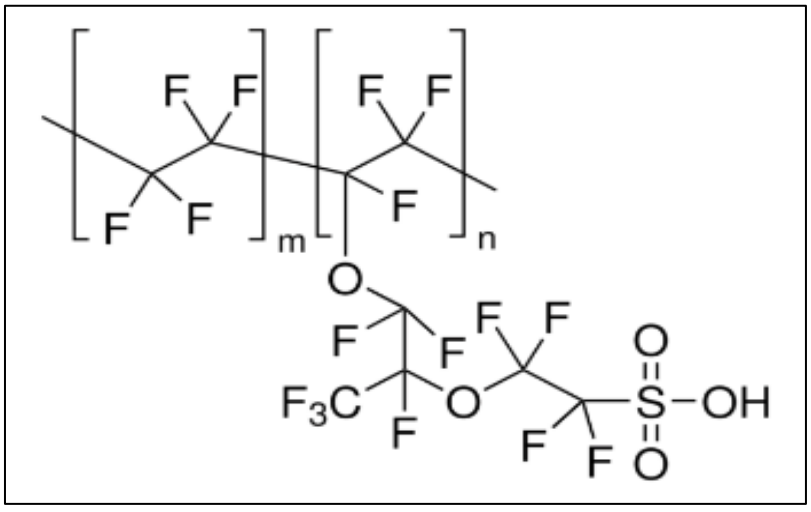

Fig. 1 *General PFSA membrane chemical formula structure provided by Sigma-Aldrich*

J. of Science and Technology Vol. 17 No. 1 (2025) 108-120

3. Methodology

3.1 FESEM-EDX Analysis

Prior to analysis, the PFSA membrane was cut into 5 mm × 5 mm squares with a thickness of 127 µm . Each membrane sample was mounted on the stub of the FESEM sample holder to ensure optimal image acquisition. Due to the inherent conductivity of the PFSA-Nafion 115 membrane, gold sputtering was not required for direct imaging. Field Emission Scanning Electron Microscopy (FESEM) and Energy-Dispersive X-ray Spectroscopy (EDX) were performed using the Apreo 2S model by Thermo Scientific. FESEM imaging was conducted at an accelerating voltage of 2 kV with magnifications ranging from 5,000× to 40,000×. Following surface imaging, chemical elemental analysis was carried out using EDX mapping to ensure the chemical present in the matrix of the PFSA membrane [11]. For cross-sectional analysis, the membrane was vertically positioned on a dedicated cross-section stub. During FESEM-EDX scanning, backscattered electron imaging was employed to enhance material contrast and surface detail. This approach enabled precise characterization of the membrane's surface morphology and elemental composition. All procedures were conducted in accordance with ASTM E986-04 (Reapproved 2010) and FESEM ASTM (2014) standards.

3.2 Tensile Analysis

The PFSA membrane sample was carefully cut into a square measuring 2 cm × 2 cm for tensile testing. To ensure accurate measurement, the sample was securely mounted on the grips of the tensile testing apparatus. Proper alignment and firm clamping were essential to maintain uniform stress distribution across the membrane during testing. Special attention was given to prevent any slippage or distortion, which could compromise the accuracy of the results. Prior to testing, the tensile machine was calibrated and set to operate at a crosshead speed of 30 mm/min under ambient temperature conditions. The tensile strength measurements were performed using a Shimadzu AG-X Universal Testing Machine (UTM). The procedure was conducted in accordance with ASTM D4073/D4073M-06(2019) e1, the Standard Test Method for Tensile-Tear Strength of Bituminous Roofing Membranes, which served as the guiding standard throughout the analysis.

3.3 Thermal Stability Testing by TGA Analysis

The PFSA membrane sample was precisely cut into a 2 cm × 2 cm square for tensile testing. To ensure accurate results, the sample was firmly secured in the grips of the tensile testing machine, with careful attention to proper alignment and clamping. This setup was critical to achieve uniform stress distribution across the membrane and to prevent any slippage or deformation that could affect the test accuracy. Before testing, the tensile machine was calibrated and set to a crosshead speed of 30 mm/min under ambient temperature conditions. Tensile strength measurements were conducted using a Shimadzu AG-X Universal Testing Machine (UTM). The testing procedure followed the guidelines of ASTM D4073/D4073M-06(2019) e1, the Standard Test Method for Tensile-Tear Strength of Bituminous Roofing Membranes, which provided the framework for the analysis.

4. Results and Discussion

4.1 Morphology PFSA Membrane Analysis by FESEM-EDX

Fig 2 illustrates the integration of the PFSA membrane within an electrolyser cell. In Figure 2(A), a Field Emission Scanning Electron Microscope (FESEM) image shows the surface morphology of the PFSA membrane at 500× magnification. The membrane surface appears predominantly smooth, with minor imperfections such as surface protrusions, likely resulting from the fabrication process. Fig2(B) presents a schematic of the membrane ideal placement between the anode and cathode inside the electrolyser. This diagram highlights the membrane's critical role in the electrolysis process by facilitating proton (H^+) transfer from the anode to the cathode, while simultaneously preventing the crossover of hydrogen and oxygen gases and inhibiting electron movement within the cell. This selective functionality is essential for maintaining the efficiency, safety, and overall reliability of electrolyser operation [12].

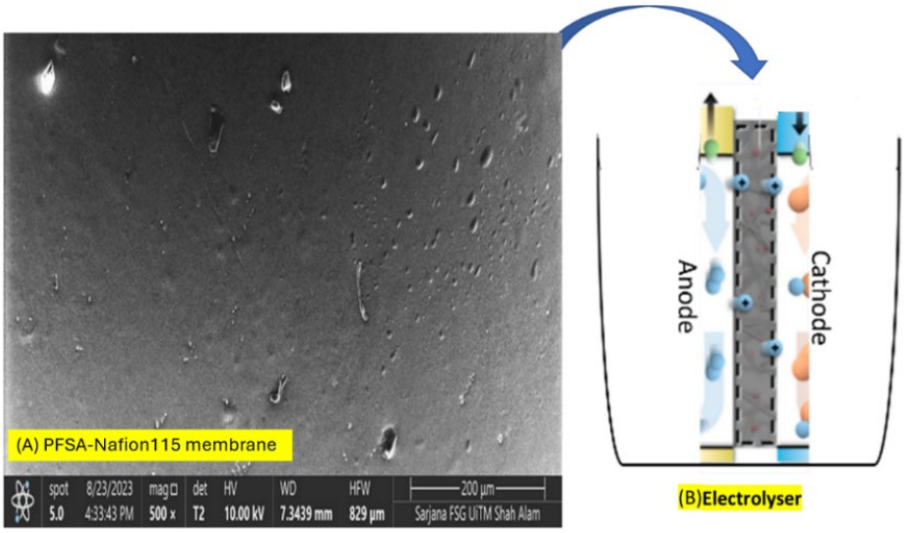

(a) **(b)**

Fig. 2 *PFSA membrane placed in between anode and cathode in electrochemical cell this observation at 200µm magnification [13]*

This FESEM imaging analysis provides crucial insights into both the physical morphology and surface elemental composition of the PFSA membrane. This analysis is vital for understanding how the membrane surface behaves and interacts during the electrolysis process within the electrolyser cell [14]. Notably, surface defects were observed in the FESEM image (Fig. 2a), indicating that the membrane morphology, particularly the presence of surface cavities, may influence electrochemical performance. These structural features can affect key properties such as proton conductivity and membrane durability[15]. Further reported that modifying Nafion membranes with additional materials, such as polyphenylsulfone, can significantly improve conductivity. This enhancement is attributed to the increased water retention capability of the composite membrane, which supports more efficient proton transport[16].

Fig. 2b illustrates the functional placement of the PFSA membrane within an electrolyzer cell, emphasizing its critical role in separating the electrodes and facilitating transport. Together, Fig. 2a and 2b provide a comprehensive overview of the membrane's application, combining both microstructural analysis and its integration within an electrochemical system. This highlights the importance of membrane properties in optimizing the design and operation of electrochemical energy conversion devices[17]. The PFSA membrane is considered a leading candidate for electrolyzer applications, as it effectively supports hydrogen gas generation by enabling the dissociation of water into protons and electrons in the presence of a catalyst[18].

Fig. 3 presents four FESEM images of the PFSA membrane captured at different magnifications, providing a detailed analysis of its surface morphology. Images 3a and 3b were obtained at magnifications of 1,000× and 4,000×, respectively, allowing for the observation of fine surface features such as particle distribution and structural uniformity. The increasing magnification reveals the membrane relatively smooth surface with the presence of uniformly dispersed particulate matter, indicative of its consistent morphology and material integrity.

J. of Science and Technology Vol. 17 No. 1 (2025) 108-120

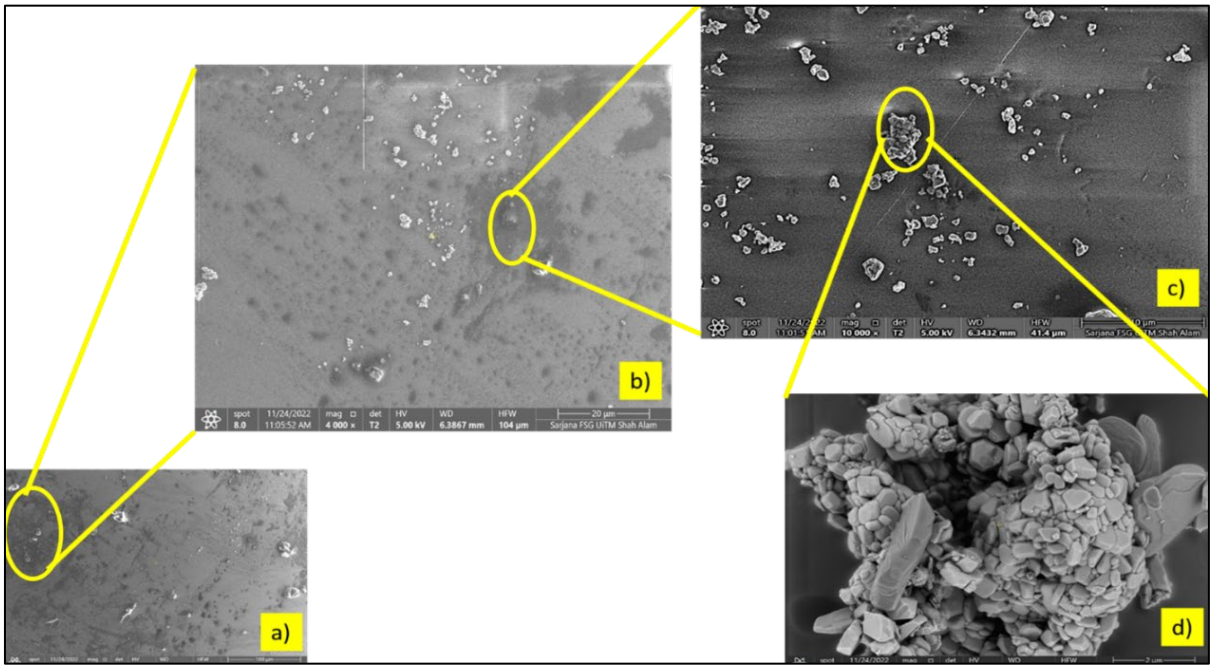

Fig. 3 *Represent PFSA membrane morphology with magnification 1k (a) 1k; (b) 4k; (c) 10k; and (d) 40k*

Fig. 3c presents the PFSA membrane surface at a magnification of 10,000×, allowing for clearer observation of surface particles and subtle morphological variations. At the maximum magnification of 40,000×, shown in Image 3d, the membrane structure is depicted in greater detail, revealing the shape, size, and distribution of particles, including both isolated and clustered forms. These morphological features are critical, as they influence key membrane properties such as proton conductivity and mechanical stability, both of which directly affect the overall performance and efficiency of the electrolyzer system[19].

Fig. 4 presents high-magnification FESEM images of the PFSA membrane, revealing progressively detailed surface characteristics. At lower magnifications (1,000× and 4,000×), the membrane exhibited a generally uniform surface with some observable defects and particle distribution. As the magnification increased to 10,000× and 40,000×, finer morphological features became more apparent, including the structure, shape, and arrangement of surface particles. This detailed morphological analysis provides critical understanding into the membrane attributes, including the presence of fractures, fissures, particle distribution, and surface composition. These factors are essential for evaluating its electrochemical performance [20] .

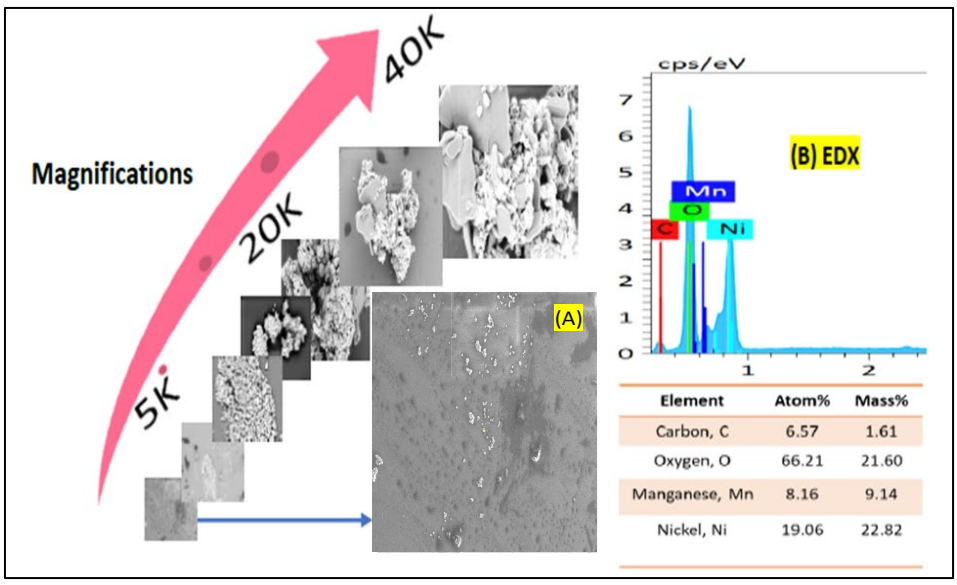

Fig. 4 *FESEM images and EDX analysis of PFSA-Nafion115 membrane at 5K, 20K and 40 K magnifications and EDX analysis was observed at 5K magnification*

Fig. 4 presents a series of scanning electron microscopy (SEM) images of the PFSA membrane. Fig. 4A was captured at varying magnifications using field emission scanning electron microscopy (FESEM), while Fig. 4B displays the corresponding energy-dispersive X-ray spectroscopy (EDX) analysis. The FESEM images were obtained at magnifications of 5,000× (5k), 20,000× (20k), and 40,000× (40k) to examine the membrane's surface morphology in increasing detail. At 5k magnification, the membrane surface appears relatively smooth, with some dispersed particulate matter. At 20k, the particles become more defined and appear to form clustered structures. At the highest magnification of 40k, individual particles are distinctly visible, offering a clearer view of their shape and distribution. This morphological characterization provides valuable insights into the surface features of the PFSA membrane, which are likely influenced by the physicochemical interactions within the matrix during its fabrication and operational processes [21].

At highest magnification, the surface features of the PFSA membrane become more visible, exposing the nano-scale texture that could potentially impact the membrane characteristic. The finding of manganese (Mn) and nickel (Ni) indicates the potential catalyst mechanism and suspects of additives which intended to improve the performance of PFSA membrane. The purposes of enhancement during PFSA membrane manufacturing stage were targeted applications related to electrochemical devices such as fuel cells or electrolyzers. This integration of FESEM and EDX investigations provides a thorough comprehension of the material properties of the PFSA membrane by encompassing its surface morphology and elemental composition. These factors are crucial in assessing its suitability and effectiveness in targeted application [22]. Instead of FESEM, EDX analysis offers a precise evaluation of the elemental composition which is essential to comprehend the chemical characteristics and potential reactivity of the membrane.

The EDX analysis shows fig. 2(B) represents the spectrum corresponding to the different elements detected on the PFSA membrane scanning. The results indicate that based on the element composition, the highest atomic percentage is oxygen (66.21%), indicating a significant presence on the membrane surface, followed by nickel (19.06%), manganese (8.16%), and carbon (6.57%). Then, based on mass percentage, Nickel has the highest mass percentage (22.82%), while it is not the most abundant element in terms of atoms, it is heavier than the other elements present. Oxygen, despite having the highest atomic percentage, has a lower mass percentage (21.60%) compared to nickel. The present of nikel (Ni) in PFSA membrane is due to behavior of nikel based catalyst enhancing durability and sustaining high operational metric for water electrolysis and overall system[23].

Due to their unique structural and functional qualities, commercial perfluorosulfonic acid (PFSA) membranes widely used in electrochemical applications such as flow batteries and electrolysers. The membranes are made up of a polytetrafluoroethylene (PTFE) backbone that doesn't like water and hydrophilic side chains that end in sulfonic acid groups ($-SO_0H$) (refer to fig 1)[24]. In wet conditions, the interaction between these domains creates a clear cluster-network structure with ionic clusters. This structure makes it easy for protons to move quickly using both the Grotthuss mechanism (proton hopping) and the vehicular mechanism (proton movement with water molecules) [25].The EDX analysis shown in Figure 4B confirms the idea that the PFSA membrane surface has oxygen-rich functional groups. These groups are necessary to maintain the membrane hydrated and allow for high ionic conductivity. In addition, the high oxygen level seen is linked to the sulfonic acid groups and the ability to take in water, which are both important for proton conduction to work well [26]. Finding elements like nickel and manganese, which were probably added when the membrane was being made or when the catalyst was being integrated, shows that the membrane could have better electrochemical performance[27].

The backbone made of PTFE helps the membrane stay chemically stable even in harsh working situations. Even with these benefits, however, the high cost of making PFSA membranes is still a big reason why they aren't widely used in energy storage and conversion systems. Combining FESEM and EDX research shows the surface topography and elemental make-up. Knowing these details is important for improving membrane design and lowering production costs without affecting performance.[28]

4.2 Cross Section of PFSA membrane Analysis

Fig. 5 illustrates the cross-sectional morphology of the PFSA membrane was obtained through Field Emission Scanning Electron Microscopy (FESEM) at a magnification of 1,000. The image illustrates the internal structural characteristics of the membrane, exhibiting a measured thickness of approximately 130 μm. This measurement value aligns with the standard thickness specifications for commercially PFSA membranes [29]. The cross-sectional view reveals a dense, compact membrane structure with embedded particulate materials predominantly located along the upper surface region. The distribution of these surface-deposited particles is uneven and may relate to catalyst loading, membrane-electrode assembly processes, or residual inorganic components from membrane activation or conditioning treatments[30]. Their presence may affect the interfacial properties of the membrane, such as ion exchange capacity, surface conductivity, and interactions with electrode materials. The internal matrix of the membrane remains intact, showing no signs of delamination or structural failure, which shows mechanical robustness[31]. Although the discovered microvoids images within the membrane interior, this may be related to hydration domains or leftover manufacturing stresses, but the membrane overall integrity does

not appear to be affected[32]. This morphological characterisation offers essential understandings into the structural uniformity and functional surface behaviour of the PFSA membrane which underscoring its appropriateness for electrochemical applications like electrolysers. Adequate thickness, dense morphology, and controlled surface particle distribution are critical for ensuring high proton conductivity, mechanical stability, and sustained performance under operational conditions [33].

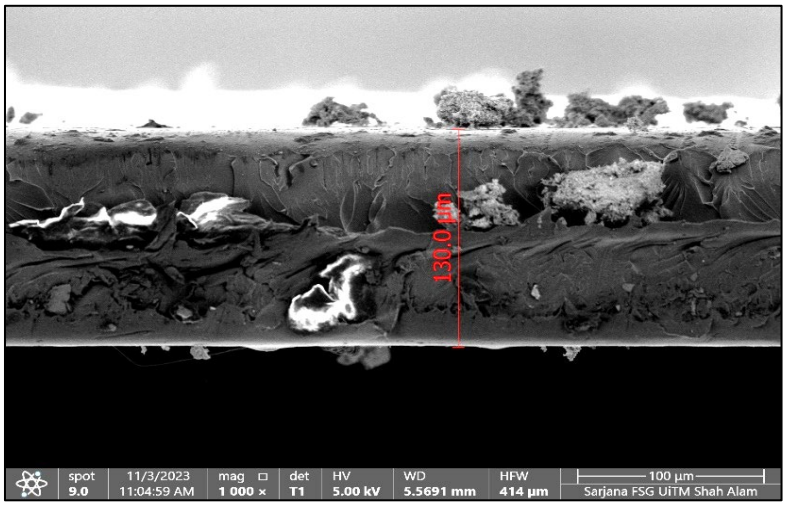

Fig. 5 *Cross section of PFSA membrane*

4.3 EDX Cross Section of PFSA-Nafion115 Membrane Analysis

The spectrum of EDX analysis shows that the PFSA membrane cross section in Fig. 6 displayed the individual peaks that correspond to the different elements present in membrane. The spectrum shows y-axis represents the intensity of X-ray emissions produced by each element resulted from excitement by the electron beam and it is measured in counts per second per electron volt (cps/eV).This analysis represent the chemical elemental in PFSA membrane as in the peaks labelled as chemical symbols used to indicate each peak according to their individual elements which are fluorine (F), carbon (C), oxygen (O), sulphur (S), and titanium (Ti) [34].

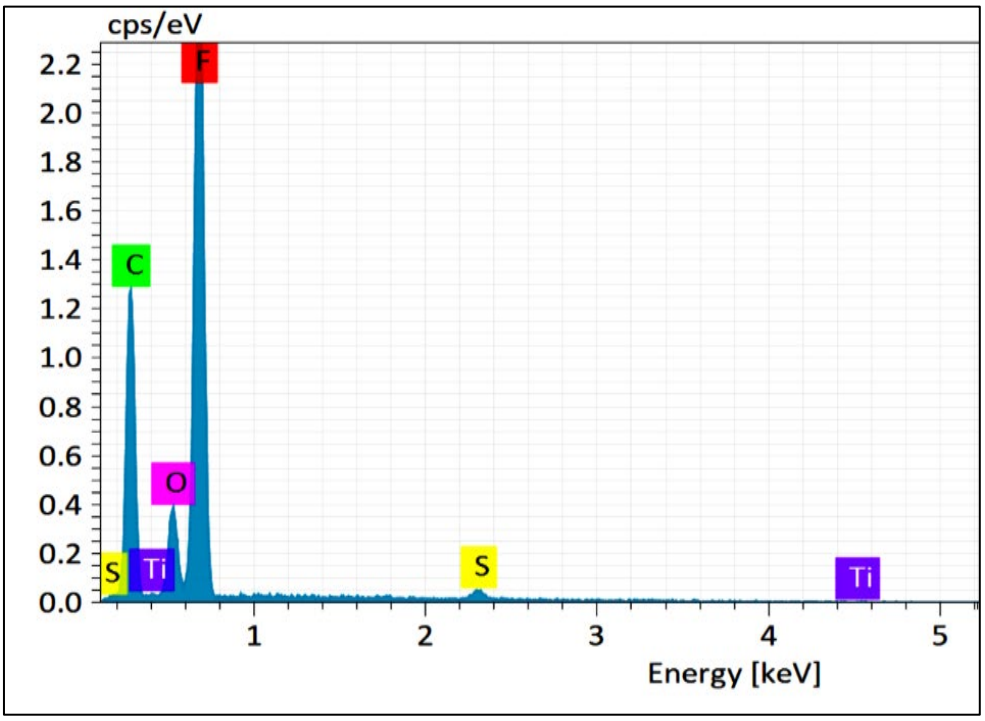

Fig. 6 *EDX analysis peaks of surface elements of cross section PFSA membrane*

Table 1 displays the elements together with their corresponding mass percentages (%) and atomic percentages (%). Fluorine (F) has the highest mass percentage of 60.71% and atomic percentage of 53.51%. This revealed the PFSA membrane possessed the majority with fluoropolymer. Carbon (C) is the second most prevalent element of both mass and atomic percentages at 25.27% and 35.24% respectively. Oxygen (O) constitutes 8.40% of the mass and 8.79% of the atomic percentage. Sulphur (S) and titanium (Ti) are found in smaller quantities, comprising 2.82% and 2.80% of the total mass, and 1.47% and 0.98% of the total atomic composition, respectively. Florine (F) is found in the PFSA membrane because of a widely recognized material used for various electrochemistry applications [35]. This PFSA was sulfonated tetrafluoroethylene-based fluoropolymer-copolymer which is owned better in physical-chemical stability and high ionic conductance at moderate operating temperatures [36].

Table 1 *EDX chemical element analysis of PFSA membrane*

Element	Mass %	Atom %
Fluorine (F)	60.71	53.51
Carbon (C)	25.27	35.24
Oxygen (O)	8.40	8.79
Sulfur (S)	2.82	1.47
Titanium (Ti)	2.80	0.98

The PFSA membrane chemical composition, obtained through Energy-Dispersive X-ray Spectroscopy (EDX), is crucial for its electrochemical behaviours and suitability for applications like fuel cells and water electrolysers [37] . The high fluorine content confirms a perfluorinated backbone, a signature feature of PFSA membranes. The presence of sulphur (S) and titanium (Ti) may indicate the presence of catalytic or reinforcement additives. The FESEM cross-sectional view allows for a deeper understanding of the membrane morphology, with particulate distributions indicating metallic elements like Ti. These findings support the continued use and optimization of PFSA membranes in advanced technologies[38].

4.4 Tensile Testing for PFSA Membrane

TGA measures weight loss of a specimen as a function of temperature, thereby providing insights into its thermal decomposition behaviour. Fig. 7 presents a stress-strain curve obtained from a tensile analysis performed on a PFSA membrane. Tensile testing is destructive testing that was conducted to analyze the physical characteristics of a material and determine its properties based on temperature stability. This method is critical for examining various stages of thermal degradation, which is vital for understanding the endurance and performance of PFSA in applications such as membranes for fuel cells, where thermal stability is essential for functionality under operating conditions[39][40].

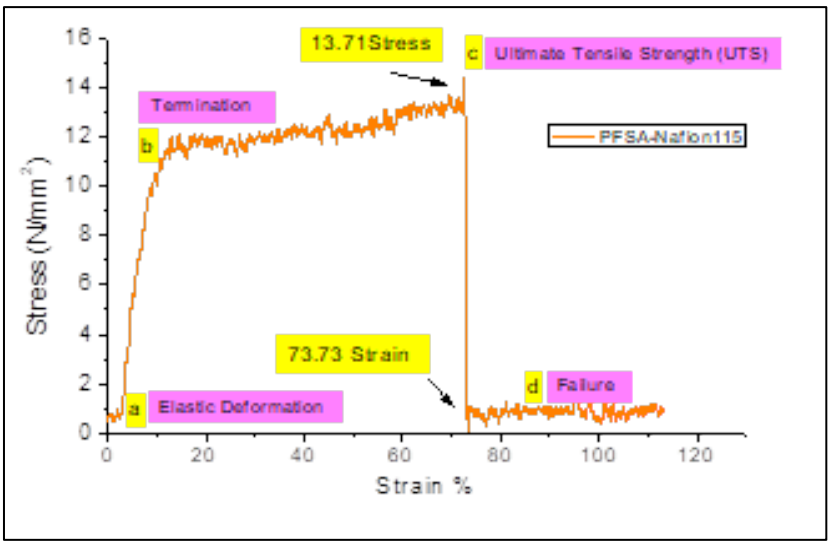

Fig. 7 *Tensile of PFSA membrane*

J. of Science and Technology Vol. 17 No. 1 (2025) 108-120

The curve reveals at point (a) as Elastic Deformation which corresponds to the initial linear component of the curve. At point (a) time, the membrane undergoes elastic deformation condition. In this locality, the substance will revert to its initial form once the burden is lifted. At point (a) to (b), the gradient of area corresponds to the Young's modulus of the substance, which quantifies its rigidity. Point at (b) indicates as Yield Point which marks as termination of the linear region where the curve begins to plateau. At this point the membrane undergoes plastic determination. The actual condition indicates that it will not revert to initial shape once the load is released. Then, the region labelled at (c) on the curve corresponds to the ultimate tensile strength (UTS) of the PFSA membrane. This condition considered as the highest level of stress that the membrane can endure and stretch before it fractures. The Ultimate Tensile Strength (UTS) of this material is specified as 13.71 N/mm^2. This value is contradicted from which the tensile strength of pure PFSA membrane is 38.2 N/mm^2 [41]. This value is higher than PFSA membrane is may due to electrostatic cross-linking. At last point, Region at (d) indicates as Failure. Then, the sudden decrease in stress indicates the precise location where the membrane experiences a fracture [42]. The strain of failure is recorded at 73.73%, showing that the membrane experienced substantial elongation prior to fracturing.

This tensile testing of PFSA membrane demonstrates elastic properties at low level of strain value (<73.73 %), which transition to plastic deformation and ultimately experiencing failure at high levels of strain (> 73.73%). The ultimate tensile strength (UTS) of 13.71 N/mm^2 and the strain at failure of 73.73% indicate that the PFSA membrane possesses a notably high resistance on stretching and endured significant elongation before fracturing. This characteristic is an advantage to enhance the durability and performance of the membrane strength [43]. Fig.8 illustrates a linear graphical depiction of the variation in force and strain over time during the tensile testing of a PFSA membrane. This analysis is helping to evaluate the mechanical of the perfluorosulfonic acid (PFSA) membrane which critically affects the performance [44].

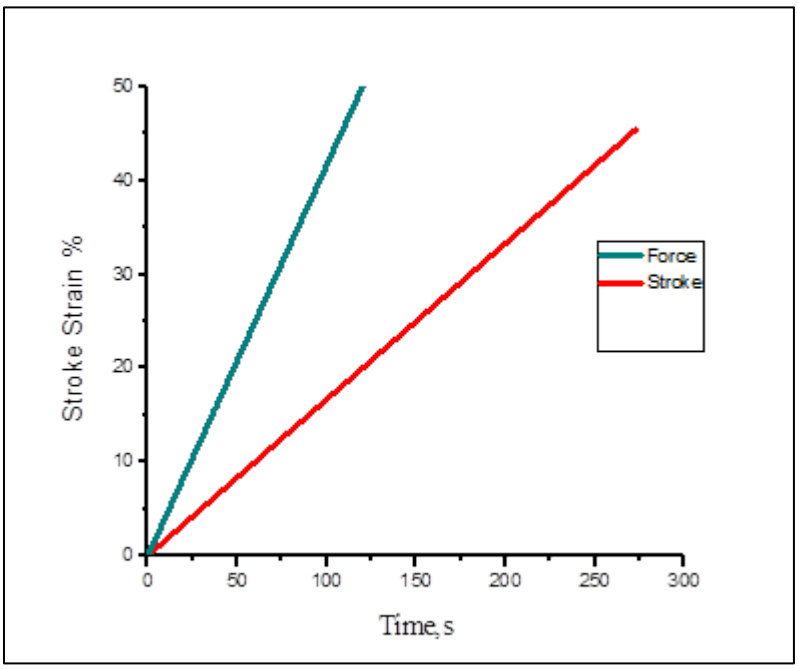

Fig. 8 *Rate analysis of force and strain during tensile testing of PFSA membrane*

The stroke linear line curve exhibits a consistent and gradual rise in stroke strain as time progresses. It indicates that the membrane undergoes consistent deformation over time until it is completed. The force line demonstrates a linear correlation with time. However, it has a more definite incline compared to the stroke line [45]. This implies that the magnitude of the force exerted on the membrane happened more rapidly than the extent of the deformation. These are the characteristics that were observed during analysis. This is caused by the membrane progressively subjected to an increasing tension, resulting in deformation. The correlation between force and stroke strain can be utilized to ascertain the characteristics which include its stiffness, ductility, and tensile strength. Thus, these tensile results offer valuable information regarding the membrane physical performance. The linear relationship between force and stroke strain over time indicates that this test was conducted with controlled conditions to systematically raise these variables at a steady rate [46].

4.5 TGA PFSA Membrane Analysis

Fig. 9 presents the Thermogravimetric Analysis (TGA) curve, demonstrating the decrease in weight of the PFSA membrane with increasing temperature. TGA is a thermal analysis method that quantifies mass loss as temperature increases, offering significant understanding into the thermal degradation characteristics of membranes. This method is commonly used to evaluate the thermal durability of PFSA membranes, which find extensive application in fuel cells and electrolysers [47]

Initially, the membrane sample maintains a stable weight. However, two distinct and rapid drops in weight are observed, indicating the occurrence of thermal decomposition at two separate temperature ranges. The first weight loss begins around 50 °C (decomposition stage 1), which can be attributed to the evaporation of water and other volatile components. A more significant weight reduction starts at approximately 300 °C, signifying the onset of decomposition and evaporation of the membrane's structural constituents [48]. The significant decomposition temperature of PFSA membranes typically occurs around 300 °C, which aligns with Decomposition Temperature 2 observed in this analysis[49]. At this stage (point b), the second major weight loss of the PFSA membrane occurs, indicating a further phase of thermal degradation involving additional membrane constituents. A final weight loss is observed at point (c), corresponding to a decomposition temperature of approximately 422 °C, representing the highest temperature before complete degradation. The derivative weight curve (%/°C) illustrates the rate of weight loss with respect to temperature. The highest peak (marked as (*)) on the curve indicates the temperature at which the membrane experiences the most rapid thermal degradation [50].

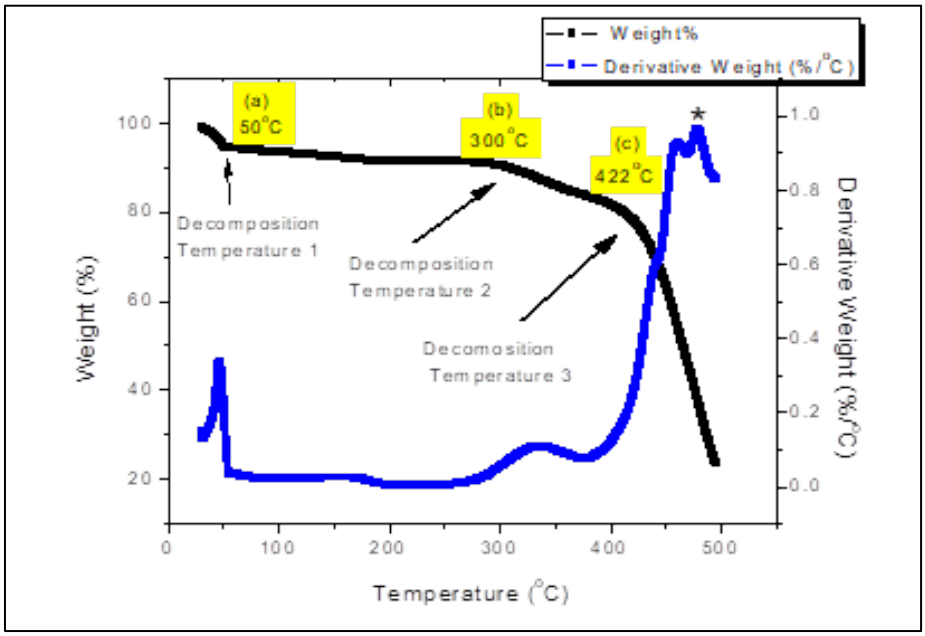

Fig. 9 *TGA analysis of PFSA-Nafion115 membrane*

The presence of three decomposition temperatures implies the membrane consists of three distinct components that exhibit varying thermal stabilities. The thermal stability of a membrane is a crucial factor in the application of fuel cells, electrolyzer and other electrochemical devices [51] [52].

5. Conclusion

This study contributes to a better understanding of the material characterisation through surface morphology study and mechanical properties of the PFSA membrane. These features are important for the membrane's efficient applications, such as in fuel cells and electrolysers in electrochemistry applications. This investigation into the surface characteristics of membrane reveals that the presence of catalyst may essential for enhancing the comprehension of the chemical present on the PFSA membrane. These results of this experimental study demonstrate additional details regarding the PFSA membrane, which is possible to be used in future applications.

Acknowledgement

The authors extend their sincere gratitude to the Malaysia Ministry of Higher Education for the generous support provided through the research grant fund under the Fundamental Research Grant Scheme (FRGS/1/2021/STG05/UITM/02/30). This funding was instrumental in the successful completion of our research

project. Additionally, the authors would like to express our appreciation to the Faculty of Applied Sciences, Universiti Teknologi MARA Malaysia, for their unwavering support throughout this work. Their commitment to fostering academic research has played a crucial role in the development and realization of our research goals.

Conflict of Interest

Authors declare that there is no conflict of interest regarding the publication of the paper.

Author Contribution

Study conception and design: *Mohd Hafiz Md ali ; Mohammad Noor Jalil* ***data collection:*** *Mohd Hafiz Md Ali;* ***analysis and interpretation of results:*** *Mohd Hafiz Md Ali, Mohammad Noor Jalil, Mohamad Nor Amirul Azhar Kamis, Hamizah Mohd Zaki;* ***draft manuscript preparation:*** *Mohd Hafiz Md Ali, Mohamad Nor Amirul Azhar Kamis. All authors reviewed the results and approved the final version of the manuscript.*

References

[1] G. Palanisamy, T. Sadhasivam, W.-S. Park, S. T. Bae, S.-H. Roh, and H.-Y. Jung, "Tuning the ion selectivity and chemical stability of a biocellulose membrane by PFSA ionomer reinforcement for vanadium redox flow battery applications," *ACS Sustain. Chem. Eng.*, vol. 8, no. 4, pp. 2040–2051, Feb. 2020. https://doi.org/10.1021/acssuschemeng.9b06631

[2] L. Li *et al.*, "Preparation and study on H–MoS2/SLS modified SPI@SPEEK blend proton exchange membrane with balanced proton conductivity and stability," *Int J Hydrogen Energy*, vol. 72, pp. 9–19, Jun. 2024, https://doi.org/10.1016/j.ijhydene.2024.04.280

[3] G. Paixão da Costa, D. M. E. Garcia, T. H. Van Nguyen, P. Lacharmoise, and C. D. Simão, "Advancements in printed components for proton exchange membrane fuel cells: A comprehensive review," *Int J Hydrogen Energy*, vol. 69, pp. 710–728, Jun. 2024,https://doi.org/10.1016/j.ijhydene.2024.05.072

[4] N. Liu *et al.*, "Nanofiber-based polymer electrolyte membranes for fuel cells," *Carbon Energy*, vol. 7, no. 4, Apr. 2025, https://doi.org/10.1002/cey2.677

[5] K. Cai *et al.*, "The incorporation of sulfonated PAF enhances the proton conductivity of Nafion membranes at high temperatures," *Polymers (Basel)*, vol. 16, no. 15, p. 2208, Aug. 2024, https://doi.org/10.3390/polym16152208

[6] J. Bin, J. Peng, W. Liu, H. Huang, L. Wang, and J. Luo, "Achieving high cell performance based on block copolymer PBI membrane with strong acid absorbing Py-PBI segments," *J Memb Sci*, vol. 709, p. 123111, Sep. 2024,https://doi.10.1016/J.MEMSCI.2024.123111

[7] X. Ren, E. Gobrogge, and F. L. Beyer, "States of water in recast Nafion® films," *J Memb Sci*, vol. 637, p. 119645, Nov. 2021, https://doi.org/10.1016/j.memsci.2021.119645

[8] T. Sharma, U. Adhikari, A. Nandimath, and J. Pandey, "Investigating degradation & mitigation strategies for proton conducting membrane in proton exchange membrane fuel cell: An approach to develop an active & stable membrane," *Materials Today Sustainability*, vol. 30, p. 101103, Jun. 2025, https://doi.10.1016/J.MTSUST.2025.101103

[9] T. Al Rafei, N. Y. Steiner, E. Pahon, and D. Hissel, "Polymer electrolyte membrane fuel cell for medium- and heavy-duty vehicles: An opportunity for commercialization," *Energy Conversion and Management: X*, vol. 27, p. 101070, Jul. 2025, https://doi.10.1016/J.ECMX.2025.101070

[10] A. Ali, N. Zhang, and R. M. Santos, "Mineral characterization using scanning electron microscopy (SEM): A review of the fundamentals, advancements, and research directions," *Appl. Sci. (Basel)*, vol. 13, no. 23, p. 12600, Nov. 2023, https://doi.org/10.3390/app132312600

[11] M. M. Ba-Abbad, N. Mahmud, A. Benamor, E. Mahmoudi, M. S. Takriff, and A. W. Mohammad, "Improved properties and salt rejection of polysulfone membrane by incorporation of hydrophilic cobalt-doped ZnO nanoparticles," *Emergent Mater.*, vol. 7, no. 2, pp. 509–519, Apr. 2024. https://doi.org/10.1007/s42247-023-00613-w

[12] S. R. F. Lala and S. Shahgaldi, "Mass and charge transport phenomena in porous transport layer for proton exchange membrane water electrolyzers: A review," *Energy Reports*, vol. 13, pp. 162–183, Jun. 2025, https://.doi.10.1016/J.EGYR.2024.11.089

[13] M. Kim, H. Ko, S. Y. Nam, and K. Kim, "Study on control of polymeric architecture of sulfonated hydrocarbon-based polymers for high-performance polymer electrolyte membranes in fuel cell applications," Oct. 01, 2021, *MDPI*. https://.doi.10.3390/polym13203520

[14] S. N. N. M. Makhtar, N. K. A. Hamed, and M. A. H. bin Hamdan, "Morphological analysis of photocatalytic membrane (SEM, FESEM, TEM)," *Advanced Ceramics for Photocatalytic Membranes: Synthesis Methods, Characterization and Performance Analysis, and Applications in Water and Wastewater Treatment*, pp. 221–238, Jan. 2024, https://doi.10.1016/B978-0-323-95418-1.00006-9

[15] J. Fu *et al.*, "Highly proton conductive and mechanically robust SPEEK composite membranes incorporated with hierarchical metal–organic framework/carbon nanotubes compound," *Journal of Materials Research and Technology*, vol. 22, pp. 2660–2672, Jan. 2023, https://.doi.10.1016/J.JMRT.2022.12.118
[16] B. Barik *et al.*, "Highly enhanced proton conductivity of single-step-functionalized graphene oxide/nafion electrolyte membrane towards improved hydrogen fuel cell performance," *Int J Hydrogen Energy*, vol. 48, no. 29, pp. 11029–11044, Apr. 2023, https://doi.10.1016/J.IJHYDENE.2022.12.137
[17] E. Y. Safronova, D. Y. Voropaeva, A. A. Lysova, O. V Korchagin, V. A. Bogdanovskaya, and A. B. Yaroslavtsev, "On the properties of Nafion membranes recast from dispersion in N-methyl-2-pyrrolidone," *Polymers (Basel)*, vol. 14, no. 23, p. 5275, Dec. 2022.
[18] Y. D. Herlambang *et al.*, "Application of a PEM Fuel Cell Engine as a Small-Scale Power Generator for Small Cars With Different Fuel Concentrations," 2023. https://.doi.10.31603/ae.9225
[19] E. E. Nzaba Madila, A. Makhsoos, M. M. Shanbhag, and B. G. Pollet, "Advancements in electrolyser stack performance: A comprehensive review of Latest technologies and efficiency strategies," *Int J Hydrogen Energy*, Apr. 2025, https://.doi.0.1016/J.IJHYDENE.2025.04.047
[20] S. Pourziad, M. R. Omidkhah, and M. Abdollahi, "Preparation of fouling-resistant and self-cleaning PVDF membrane via surface-initiated atom transfer radical polymerization for emulsified oil/water separation," *Can. J. Chem. Eng.*, vol. 97, no. S1, pp. 1581–1588, Jun. 2019, https://doi.org/10.1002/cjce.23372
[21] C. Shang, D. Pranantyo, and S. Zhang, "Understanding the Roughness–Fouling Relationship in Reverse Osmosis: Mechanism and Implications," 2020. https://doi.10.1021/acs.est.0c00535
[22] S. S. Karim, S. Farrukh, A. Hussain, M. Younas, and T. Noor, "The influence of polymer concentration on the morphology and mechanical properties of asymmetric polyvinyl alcohol (PVA) membrane for O_2/N_2 separation," *Polym. Polym. Compos.*, vol. 30, p. 096739112210900, Jan. 2022. https://doi.org/10.1177/09673911221090053
[23] Z. Angeles-Olvera, A. Crespo-Yapur, O. Rodr\'\iguez, J. Cholula-D\'\iaz, L. Mart\'\inez, and M. Videa, "Nickel-based electrocatalysts for water electrolysis," *Energies (Basel)*, vol. 15, no. 5, p. 1609, Feb. 2022. https://doi.org/10.3390/en15051609
[24] E. Y. Safronova, A. A. Lysova, D. Y. Voropaeva, and A. B. Yaroslavtsev, "Approaches to the modification of perfluorosulfonic acid membranes," *Membranes (Basel)*, vol. 13, no. 8, Aug. 2023. https://doi.org/10.3390/membranes13080721
[25] C. Li and G. A. Voth, "A quantitative paradigm for water-assisted proton transport through proteins and other confined spaces," *Proc. Natl. Acad. Sci. U. S. A.*, vol. 118, no. 49, p. e2113141118, Dec. 2021. https://doi.org/10.1073/pnas.2113141118
[26] R. R. R. Sulaiman, R. Walvekar, W. Y. Wong, M. Khalid, and M. M. Pang, "Proton conductivity enhancement at high temperature on polybenzimidazole membrane electrolyte with acid-functionalized graphene oxide fillers," *Membranes (Basel)*, vol. 12, no. 3, p. 344, Mar. 2022. https://doi.org/10.3390/membranes12030344
[27] J. R. Tumiwa and T. Mizik, "Advancing nickel-based catalysts for enhanced hydrogen production: Innovations in electrolysis and catalyst design," *Int J Hydrogen Energy*, vol. 109, pp. 961–978, Mar. 2025, doi: 10.1016/J.IJHYDENE.2025.02.020.
[28] L. Hu *et al.*, "Ion/Molecule-selective transport nanochannels of membranes for redox flow batteries," *Energy Storage Mater*, vol. 34, pp. 648–668, Jan. 2021, https://.doi.10.1016/J.ENSM.2020.10.008
[29] R. Ohno, K. Shudo, T. Tano, and K. Kakinuma, "Development of polymer composite membranes with hydrophilic TiO_2 nanoparticles and perfluorosulfonic acid-based electrolyte for polymer electrolyte fuel cells operating over a wide temperature range," *ACS Appl. Energy Mater.*, vol. 6, no. 19, pp. 10098–10104, Oct. 2023. https://doi.org/10.1021/acsaem.3c01721
[30] S. Hegde, R. Wörner, and B. Shabani, "Automotive PEM fuel cell catalyst layer degradation mechanisms and characterisation techniques, Part I: Carbon corrosion and binder degradation," *Int J Hydrogen Energy*, vol. 118, pp. 268–299, Apr. 2025, https://.doi.0.1016/J.IJHYDENE.2025.02.402
[31] R. McNair, G. Szekely, and R. A. W. Dryfe, "Ion-exchange materials for membrane capacitive deionization," *ACS ES T Water*, vol. 1, no. 2, pp. 217–239, Feb. 2021. https://doi.org/10.1021/acsestwater.0c00123
[32] S. Alsoy Altinkaya, "A review on microfiltration membranes: fabrication, physical morphology, and fouling characterization techniques," *Front. Membr. Sci. Technol.*, vol. 3, Jul. 2024. https://doi.org/10.3389/frmst.2024.1426145
[33] P. Hasanzade, P. Gharbani, and B. M. Derakhshan Fahime and Maher, "Preparation and characterization of PVDF/g-C_3N_4/chitosan nanocomposite membrane for the removal of Direct Blue 14 dye," Feb. 2021. https://doi.org/10.21203/rs.3.rs-218812/v1
[34] M. M. Tellez-Cruz, J. Escorihuela, O. Solorza-Feria, and V. Compañ, "Proton exchange membrane fuel cells (PEMFCs): Advances and challenges," *Polymers (Basel)*, vol. 13, no. 18, p. 3064, Sep. 2021. https://doi.org/10.3390/polym13183064

[35] M. Adamski, N. Peressin, and S. Holdcroft, "On the evolution of sulfonated polyphenylenes as proton exchange membranes for fuel cells," *Mater. Adv.*, vol. 2, no. 15, pp. 4966–5005, 2021. https://doi.org/10.1039/D1MA00511A
[36] O. Kwon, J. Park, and J. Lee, "Quantitative Study of Charge Distribution Variations on Silica–Nafion Composite Membranes Under Hydration Using an Approximation Model," 2023. https://.doi.10.3390/polym15102295
[37] M. Nara *et al.*, "Evaluating cation-exchange membrane properties affecting polymer electrolyte membrane water electrolysis," *ACS Omega*, vol. 10, no. 10, pp. 10425–10431, Mar. 2025. https://doi.org/10.1021/acsomega.4c10548
[38] V. A. Paganin, A. M. P. Sakita, T. Lopes, E. A. Ticianelli, and J. Perez, "Uncovering key parameters in perfluorosulfonic acid (PFSA) membrane fuel cells to enhance performance," *Membranes (Basel)*, vol. 15, no. 3, Feb. 2025. https://doi.org/10.3390/membranes15030065
[39] N. Saba, M. Jawaid, and M. T. H. Sultan, "An overview of mechanical and physical testing of composite materials," *Mechanical and Physical Testing of Biocomposites, Fibre-Reinforced Composites and Hybrid Composites*, pp. 1–12, Jan. 2019, https://.doi.10.1016/B978-0-08-102292-4.00001-1
[40] P. Giani and S. Locarno, "Tensile testing of polymeric materials: a model-based approach to estimate the material strength without position sensor," *J. Phys. D Appl. Phys.*, vol. 58, no. 7, p. 75301, Feb. 2025. https://doi.org/10.1088/1361-6463/ad9615
[41] Y. Tang, A. M. Karlsson, M. H. Santare, M. Gilbert, S. Cleghorn, and W. B. Johnson, "An experimental investigation of humidity and temperature effects on the mechanical properties of perfluorosulfonic acid membrane," *Materials Science and Engineering: A*, vol. 425, no. 1–2, pp. 297–304, Jun. 2006, https://.doi.10.1016/J.MSEA.2006.03.055
[42] Z. Liu, S. Cai, Z. Tu, and S. H. Chan, "Recent development in degradation mechanisms of proton exchange membrane fuel cells for vehicle applications: problems, progress, and perspectives," *Energy Storage and Saving*, vol. 3, no. 2, pp. 106–152, Jun. 2024, https://.doi.10.1016/J.ENSS.2024.02.005
[43] J.-H. Ho *et al.*, "Upcycling fabrics: Valorization of recycled polyethylene terephthalate (r-PET) plastic waste into thermoplastic polyester elastomers (TPEE) for fiber spinning," *ACS Appl. Polym. Mater.*, vol. 6, no. 1, pp. 552–560, Jan. 2024. https://doi.org/10.1021/acsapm.3c01943
[44] H. J. Lim, G. Kim, and G. J. Yun, "Durability and performance analysis of polymer electrolyte membranes for hydrogen fuel cells by a coupled chemo-mechanical constitutive model and experimental validation," *ACS Appl. Mater. Interfaces*, vol. 15, no. 20, pp. 24257–24270, May 2023. https://doi.org/10.1021/acsami.2c15451
[45] S. Dutta and S. Ghosh, "Analysis and design of tensile membrane structures: Challenges and recommendations," *Pract. Period. Struct. Des. Constr.*, vol. 24, no. 3, p. 4019009, Aug. 2019. https://doi.org/10.1061/(ASCE)SC.1943-5576.0000426
[46] S. Acarer *et al.*, "Characterisation and mechanical modelling of polyacrylonitrile-based nanocomposite membranes reinforced with silica nanoparticles," *Nanomaterials (Basel)*, vol. 12, no. 21, p. 3721, Oct. 2022. https://doi.org/10.3390/nano12213721
[47] E. Wallnöfer-Ogris *et al.*, "A review on understanding and identifying degradation mechanisms in PEM water electrolysis cells: Insights for stack application, development, and research," *Int J Hydrogen Energy*, vol. 65, pp. 381–397, May 2024, https://doi.org/10.1016/j.ijhydene.2024.04.017
[48] S. A. El-Sayed, T. M. Khass, and M. E. Mostafa, "Thermal degradation behaviour and chemical kinetic characteristics of biomass pyrolysis using TG/DTG/DTA techniques," *Biomass Convers. Biorefin.*, vol. 14, no. 15, pp. 17779–17803, Aug. 2024. https://doi.10.1007/s13399-023-03926-2
[49] V. A. Paganin, A. M. P. Sakita, T. Lopes, E. A. Ticianelli, and J. Perez, "Uncovering key parameters in perfluorosulfonic acid (PFSA) membrane fuel cells to enhance performance," *Membranes (Basel)*, vol. 15, no. 3, Feb. 2025. https://doi.org/10.3390/membranes15030065
[50] S. Harikrishnan and A. D. Dhass, *Thermal transport characteristics of phase change materials and nanofluids*, 1st Edition., vol. 1. Boca Raton: CRC Press, 2022. doi: https://doi.org/10.1201/9781003163633
[51] S. C. Sutradhar *et al.*, "Sulfonyl Imide Acid-Functionalized Membranes via Ni (0) Catalyzed Carbon-Carbon Coupling Polymerization for Fuel Cells," 2021. https://doi.org/10.3390/membranes11010049
[52] K. Hooshyari, B. A. Horri, H. Abdoli, M. F. Vostakola, P. Kakavand, and P. Salarizadeh, "A Review of Recent Developments and Advanced Applications of High-Temperature Polymer Electrolyte Membranes for PEM Fuel Cells," 2021. https://doi.org/10.3390/en14175440